

# Radon-gas Monitoring by Gamma-ray Measurements on the Ground for Detecting Crustal Activity Changes—Preliminary Study by Repeat Survey Method—

Tameshige Tsukuda\*

Earthquake Research Institute, University of Tokyo

## Abstract

Concentrated stresses due to deformation of the crust may generate highly compressed interstitial fluids at depths of more than several kilometers. Such fluids tend to migrate upwards through a crack system in the crust under high pressures. A mass of radon gas is considered to be discharged into the air from underground, because radon is generated from abundant radioactive uranium and radium in the crust. Its concentration in the air is increased by the compression of fluids within the crust. Therefore, the concentration of discharged radon gas in the air is one of the important indicators of crustal activity. As the emergence of radon may be random in space and time, we have to set up a dense network of observation stations. Before constructing such a network system, preliminary surveys were attempted. The presence of radon is confirmed by gamma rays released from  $^{214}\text{Bi}$ , an intermediate decay product of radon. Using a RE-100 scintillation counter, a product of Ohyo Koken Kogyo Co., Ltd., which enables data to be recorded continuously from two bands in the gamma-ray spectrum, we took measurements close to the ground surface to monitor underground radon emissions into the air. During the last 10 years, repeated continuous observations at a fixed station and on a moving automobile or train along fixed routes positively showed the validity of the method adopted in the study presented in this paper. Repeated observations at a fixed point showed a long-term increasing trend of radon concentration in Inagawa Town, Hyogo Prefecture. Mobile measurements taken aboard a Shinkansen bullet train traveling from Kyoto to Tokyo disclosed burst-like emissions of radon at such sites as near Kyoto, as well as regional variations in the intensity of radon emissions.

**Key words:** radon, crustal activity, earthquake prediction, scintillation counter, gamma rays

## 1. Introduction

Stresses in the crust change in accordance with crustal deformations due to plate motions. Concentrated stresses at some domains in the medium may not only create new microcracks and act to expand the area and/or volume of preexisting microcracks, but also drive pore fluids to flow upward through a crack network when a vent-like path occurs in the network. Tsukuda *et al.* (2005) presented some phenomena showing evidence of a near ground surface discharge of deep water originating at depths of more than several kilometers. If we monitor the ground surface, we will also detect gasses coming out

from deep underground in response to crustal activity as we do with water.

Radon gas is a candidate deep-origin gas. Radon is a radioactive element, which is generated either in the uranium decay series or thorium decay series.  $^{222}\text{Rn}$  is predominant compared to  $^{220}\text{Rn}$  (Tn). The parent of  $^{222}\text{Rn}$  is radium, whose parent is uranium. Uranium concentrations in rocks are as much as  $4\sim 6\times 10^{-6}$  g/g in weight for granite (Evans and Goodman, 1941). The following characteristics of this gas provide advantages for monitoring crustal activity: 1) it exists in a constant mass within the crust because the quantity of radon is controlled by the

\* e-mail: tsukuda@eri.u-tokyo.ac.jp (1-1-1 Yayoi, Bunkyo-ku, Tokyo 113-0032, Japan)

radiation equilibrium between generation and decay; 2) its gaseous nature enables it to migrate easily through a crack network in the crust; 3) as it is an inert gas free from chemical reactions with environmental materials, it is not trapped in the course of movement; 4) it is easy to detect due to its radioactivity; and, 5) it has a half-life of 3.8 days, which is an appropriate time-constant for detecting crustal activity changes over several days. Radon gas takes the elements  $^{222}\text{Rn}$  and  $^{220}\text{Rn}$  or tron gas.

As radon gas diffuses in the air after discharging from underground, it is preferable to monitor it in underground soil or in water from underground sources. The most effective method for monitoring radon gas is to set up a dense network of observation stations to detect radon discharged from underground. It is extremely difficult to construct such a network system at once. Before advancing this project, we should try a simple method and confirm whether the simple measurement is valid or not for our purposes. To achieve this, a survey method has been developed over more than 10 years.

For radon detection, alpha particle measurements have been conducted for soil gas or groundwater (Hatuda, 1953; Okabe, 1956). In particular, radon gas in water has been studied and precursory changes have been detected in relation to earthquakes (Ulomov *et al.*, 1971; Ten, 1980; Wakita *et al.*, 1980; Igarashi *et al.*, 1995). and Yasuoka *et al.* (2006) detected an anomalous change in atmospheric radon concentration preceding the 1995 Kobe earthquake of M7.3 using a flow-type ionization chamber. Yamauchi and Shimo (1982) tried to detect radon radioactivity in the air at a tunnel, and found burst-like emissions of radon, which often responded to crustal deformations. In addition, Yamauchi *et al.* (1988), applying a similar technique, did experiments comparing radon concentration in the air with that in the groundwater at the same tunnel, and studied how radon gas in the air is affected by rainfall etc., and how it is scattered by dispersion. Besides, gamma ray measurements detecting radon have been conducted (e.g. Nakao *et al.*, 1987; Katsura *et al.*, 1989). A scintillation counter is a simple device for detecting gamma rays. Recently, mobile devices equipped with a small-scale scintillator have become available (Araki, 1994, 1996a, 1996b).

The gamma ray method has the merit of simple

instrumentation for detecting radon in the air. The measurable quantity is the frequency of gamma-ray incidence into the scintillator. In this case, we cannot estimate the concentration of radon, but only measure the relative intensity of the concentration.

The purpose of this paper is to present a concept for monitoring radon gas concentration in the air near ground surface. We adopt the hypothesis that radon gas may come out from deep underground in response to crustal deformation and stress concentration, and that the discharging sites are located at random in space and occur intermittently in time, rather than the hypothesis that radon emissions would occur selectively in particular regions such as active faults. The leading principle of this study is to repeatedly measure gamma ray intensity in the air just above the ground surface either at a fixed point or on a vehicle moving along a fixed survey route, so that we obtain some statistical characteristics of radon emissions from underground: spatial distributions and temporal changes. As a result, we adopted the RE-100 radon emanometer manufactured and sold by Ohyo Koken Kogyo Co., Ltd., Tokyo, whose fundamental design is based on a concept presented by Araki (1994) (Fig. 1).

## 2. Method

To detect gamma rays related to radon gas concentration in the air, we use a gamma-ray spectrometer with a scintillation counter, identifying the energy level of each gamma-ray photon. If a volume of radon gas occupies the air above the ground, specific gamma rays are released during the decay process of radon generated from the parent element radium. One specific gamma ray is released from  $^{214}\text{Bi}$ , which is an intermediate decay product in the uranium decay series after radon.  $^{222}\text{Rn}$  decays with a half-life of 3.825 days into  $^{218}\text{Po}$ , and it decays into  $^{214}\text{Pb}$  with a 3.05 m half-life, and then into  $^{214}\text{Bi}$  with a 26.8 m half-life.  $^{214}\text{Bi}$  will decay with a half-life of 19.7 m, emitting gamma rays of 607 KeV. The half-lives for  $^{218}\text{Po}$ ,  $^{214}\text{Pb}$  are so short that the incidence of the 607 KeV gamma-rays from  $^{214}\text{Bi}$  implies the presence of radon in the ambient air.

A scintillation counter is the most convenient device for detecting gamma rays for our purposes. A small piece of NaI crystal is used for the scintillator. The scintillated photons are received by an electron

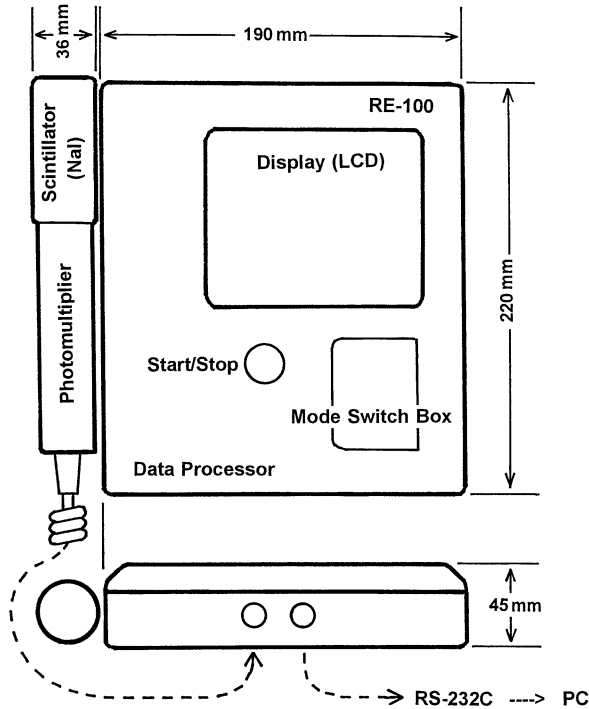


Fig. 1. Top and side views of the Radon Emanometer RE-100. Weight of the whole device is 1.6 kg including four size C batteries. The accumulated data are transmitted to a PC by a RS-232C interface cable, and used for analysis.

multiplier, which supplies electron currents in response to the incidence of gamma-ray photons. The intensity of the current for each incident event is in proportion to gamma-ray energy, and the device counts the frequency of electric current events corresponding to the incidence of gamma-ray to the scintillator for each assigned energy level.

The RE-100 gamma-ray scintillation counter (manufactured by Ohyo Koken Kogyo Co., Ltd.) is designed to count the frequency of the incidence of gamma rays in a scintillator made of crystal NaI, whose shape is a cylinder 1 inch high and 1 inch in diameter, for the respective ray energy levels (spectrum) and memorize counting data for two window channels of the spectrum. The first channel centered at 609 KeV corresponds to  $^{214}\text{Bi}$  radiation, and the second at 1.46 MeV for  $^{40}\text{K}$ . The total spectrum range is from 65 KeV to 1.6 MeV. Figure 1 illustrates the size and functions of RE-100.

Figures 2 (a) and (b) show examples of the gamma-ray spectrum, plotting the frequency of detected gamma rays against energy. The spectrum component indicating the presence of discharged radon gas

is superimposed by those of the same energy with a different origin. Some originate from space and some from the ground or other sources. How do we estimate environmental noise?

Among the noise coming from near surface rocks, gamma rays released from potassium-40 are predominant. The electron capture process of  $^{40}\text{K}$  emits 1.46 MeV gamma rays, which form a peak in the spectrum.

It was found that as the height of the peak grows the height of the low-level spectrum components also grows and has the empirical relation shown in Section 3. The spectral component of a higher level of energy will be transformed into that of a lower level of energy by Compton scattering. As illustrated in Fig. 2, radon emissions should be detected by removing background noise indicated by broken lines. The method to estimate the background level of the spectrum is discussed below.

Due to fluctuations in gamma rays detected, the spectral peak at the radiation is not so sharp that we have to set spectral windows for detection. The windows are set in the range 494–806 KeV for  $^{214}\text{Bi}$ , and 1300–1599 KeV for  $^{40}\text{K}$ . Figure 2 shows an example of measured gamma-ray spectrum, together with the two spectral windows. We estimate the count for detecting of gamma-rays in which we are interested by integrating over the width.

The spectrum in general has a high counting value at a low energy. It decreases as energy rises. This is because the high-energy gamma rays scatter and are transformed into low energy rays by the Compton effect. Thus, the count becomes higher at a low energy level than at a high energy level. The gamma rays coming from  $^{40}\text{K}$  are the main component at the high energy level in the given gamma spectrum for this instrument.

We define energy windows for the spectrum. We deal with integrated counting frequencies for each window. The integrated frequencies corresponding to  $^{214}\text{Bi}$  and  $^{40}\text{K}$  are defined by  $B$  and  $K$ , respectively. The relation between  $B$  and  $K$  is dependent on the geologic setting of the region concerned. Araki (1994) found a statistical correlation between  $B$  and  $K$  in a case without anomalous radon concentrations. We assume that when the radon concentration is normal, the two values have the functional relation:

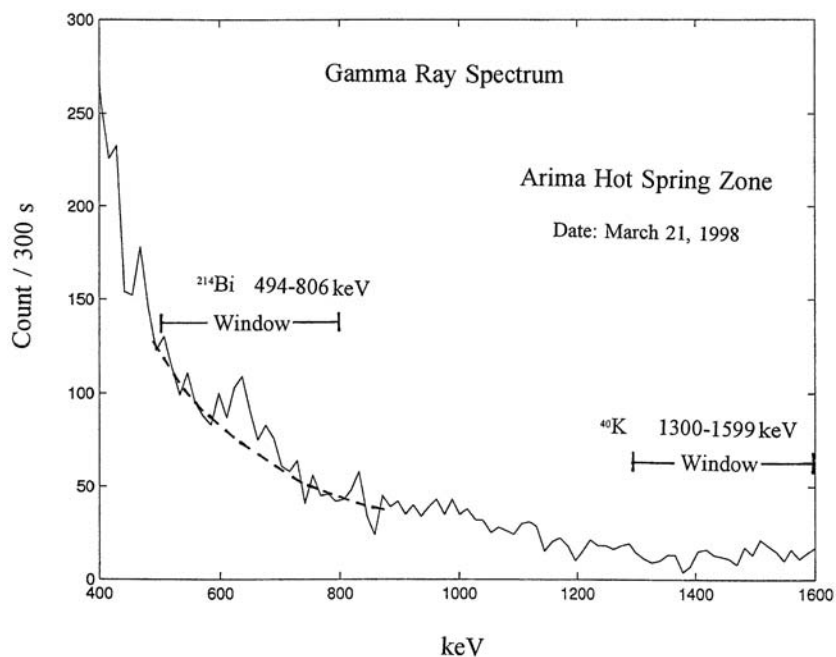


Fig. 2 (a). Gamma-ray spectrum in open air. Data are from observations in a car at Arima Hot-Spring, Kobe City, Hyogo Prefecture. Dotted line shows the assumed normal state of the spectrum. An anomaly is found at an energy level around the  $^{214}\text{Bi}$  spectral window.

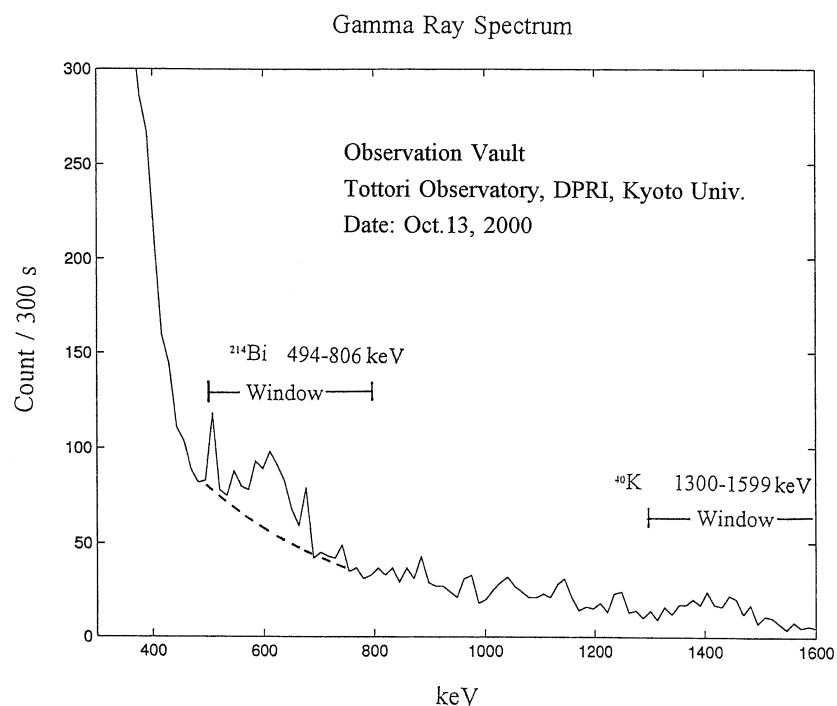


Fig. 2 (b). Gamma-ray spectrum in closed air. Data are from observations in the observational vault at Tottori Observatory, Disaster Prevention Research Institute, Kyoto University, in Tottori City. The observation vault had been used to monitor seasonal variations of radon emanations by Nakao *et al.* (1987).

$$B=f(K). \tag{1}$$

We obtain Eq. (1) empirically in the next section. It should be noted that the above function changes depending on geologic setting. An excessive radon concentration, or an anomaly, is estimated by the following calculation.

$$\delta B=B-f(K). \tag{2}$$

The excess, i.e., large supply of radon would occur for the following two reasons: one is due to a geologic setting with abundant parent elements of radon, and the other is the transportation of radon passing through cracks underground. The former case shows a relatively steady state of radon emissions without a significant temporal variation. Our aim is to get  $\delta B$  for radon indicators at many points in space and time. We call the value of  $\delta B$  the Radon Emanation Factor (*REF*) throughout this paper. If we adopt a survey route, we get one-dimensional spatial data. Next, if we repeat measurements over time, temporal data are obtained. The above method was first presented by Araki (1994, 1996a, 1996b).

In this paper, we simply define the term “radon emanation” as *REF*, the difference between the value of *B* compared to the empirical standard. Due to the adoption of an imperfectly designed function  $f(K)$  for the standard, the *REF* values are sometimes negative. We discuss the relative values of *REF* in comparison with others from different points in time or space.

### 3. Characteristics of instrument

The gamma ray detector should be easy to carry and be equipped with sufficient memory for data. RE-100 is the mobile scintillation counter equipped with a 64kB memory. This is designed so that a survey along a fault or some active zone of the crust can easily find the trace of the fault. The memorized data are modified to be read easily. This application is effective if radon gas activity is constant and the fault trace is the path for radon gas. The amount of excess radon should be an indicator for detecting an active fault trace. According to some tests preceding this study, it is doubtful if the indicator is stable for repeated measurements. Here, we concentrate our measurements on a very rough survey undertaken by automobile or train.

Table 1. Calibration of energy level of RE-100. Deviation or shift of energy level at each spectrum peak is presented in percentages.

			Gamma-ray Source			
			<sup>137</sup> Cs	<sup>60</sup> Co	<sup>60</sup> Co	KCl
Y	M	D	662 KeV	1170 KeV	1330 KeV	1461 KeV
2001	7	31	-2	-7	-8	-8
2003	6	24	-2	-8	-9	-7
2005	9	6	-8	-10	-11	-10

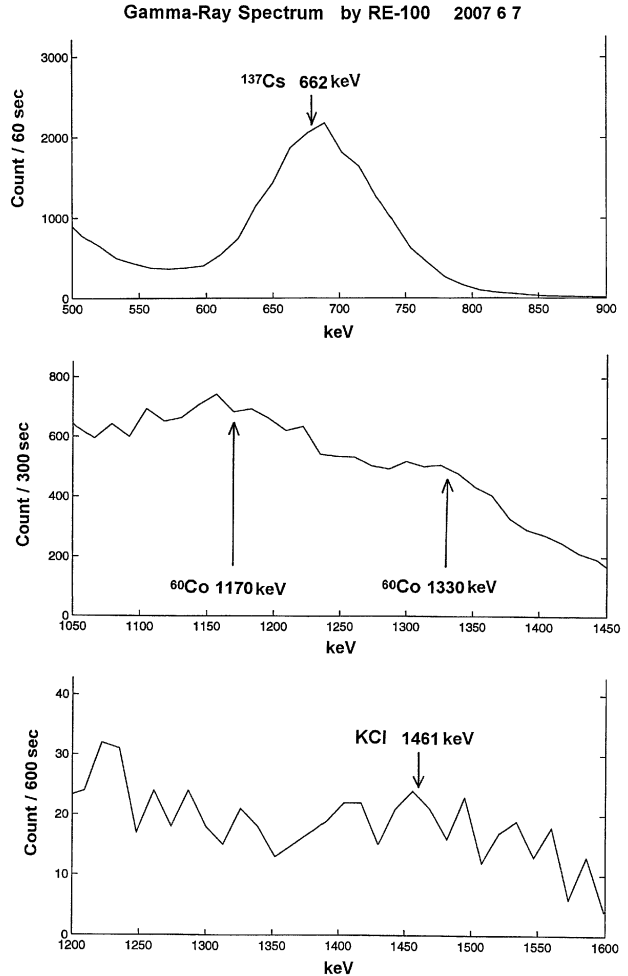


Fig. 3. Gamma-ray spectra of RE-100 for standard emitting sources, Co, Cs, and KCl for calibrating of energy levels in the gamma-ray spectrum.

RE-100 has a crystal NaI cylinder with dimensions of 2 inches in length and 1 inch in diameter. The device currently in use widely has a crystal 2 inches long and 2 inches in diameter. For ease of comparison, the gamma-ray count for RE-100 is multiplied by four for compatibility with a device having a large detector.

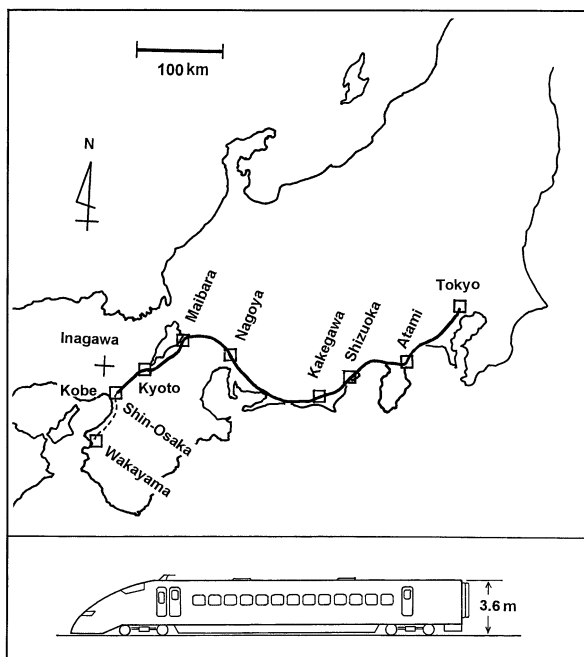


Fig. 4. Map of the Tokaido Sinkansen Line from Tokyo to Shin-Osaka and a local line (dotted line in the figure) from Shin-Osaka to Wakayama. The bottom figure is the car at the front or end of a Shinkansen-train. The radon emanometer is put on the shelf just above the top of the window of the central part of the second car from the end. It is about 3.0 m high above the rail.

Identification of a specific gamma ray is dependent on resolution and precision. A spectrum with a sharp peak and small width is preferable for identifying the gamma rays that concern us. However, the spectral pulse peak is broadened due to errors in specific gamma ray measurements. Calibration tests are conducted to maintain the precision using standard gamma-ray sources:  $^{137}\text{Cs}$  (with a peak at 662 KeV),  $^{60}\text{Co}$  (1170 KeV, 1330 KeV) and  $\text{KCl}$  for  $^{40}\text{K}$  (1461 KeV). As the test was carried out once every several years, the maximum shift from the peak on the energy spectrum is kept within 10% in this study over nearly 10 years. The measured error values in the energy level calibration are listed in Table 1. The spectral width for each spectral peak, as indicated in Fig. 3, describes resolution and precision. The width of the windows to estimate the integrated frequency of detected gamma-ray photons is designed so that the window should cover a broadened spectrum centering on the target energy level.

The original gamma-ray data measured by RE-

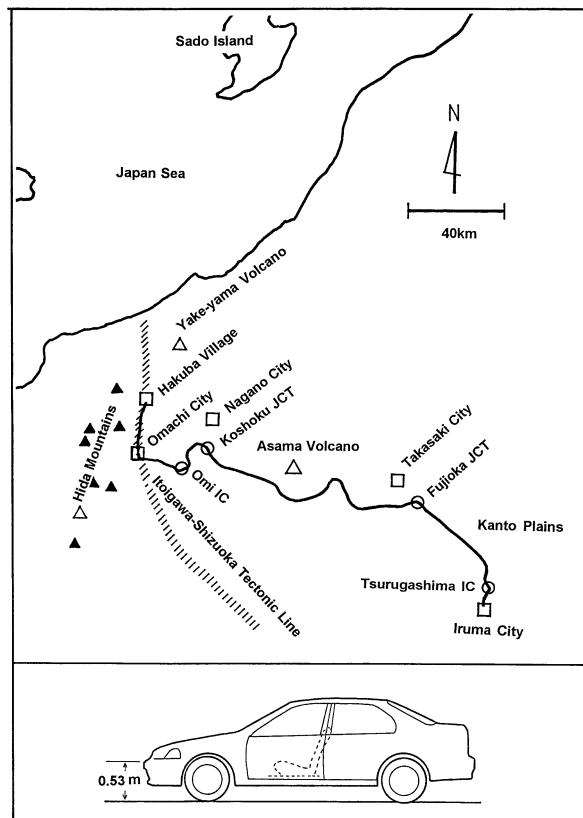


Fig. 5. Road map for gamma-ray survey undertaken by car. The radon emanometer is put on the front seat of the car. It is about 50 cm above the ground.

100 are  $K$  for  $^{40}\text{K}$  and  $B$  for  $^{214}\text{Bi}$ .  $B$  is replaced by  $\delta B$  through Eq. (2). The function  $f(K)$  in Eq. (2) is given as follows.

$$f(K) = 2.89K + 309.0 \quad (3)$$

This is an empirical relation based on data obtained at Furano, central Hokkaido (Data from Ohyo Koken Kogyo Co. Ltd.). The RE-100 radon emanometer calculates  $\delta B$  or  $REF$  immediately and memorizes it with  $K$ , and  $RATE$ , which is defined as follows:

$$RATE = -100.0\delta B / f(K). \quad (4)$$

To confirm the validity of Eq. (3), the data obtained by our measurements were analyzed estimating data  $B$  from stored data  $\delta B$ , or  $REF$  and  $RATE$ , solving Eq. (4) and Eq. (2). We can also derive  $K$  from Eq. (3). Sometimes the value obtained thus is, due to numerical errors, far from the real value originally measured. In this case, we abandon such data for the analysis. In this study, we keep the ratio of the error to the measured value of  $K$  within 1%

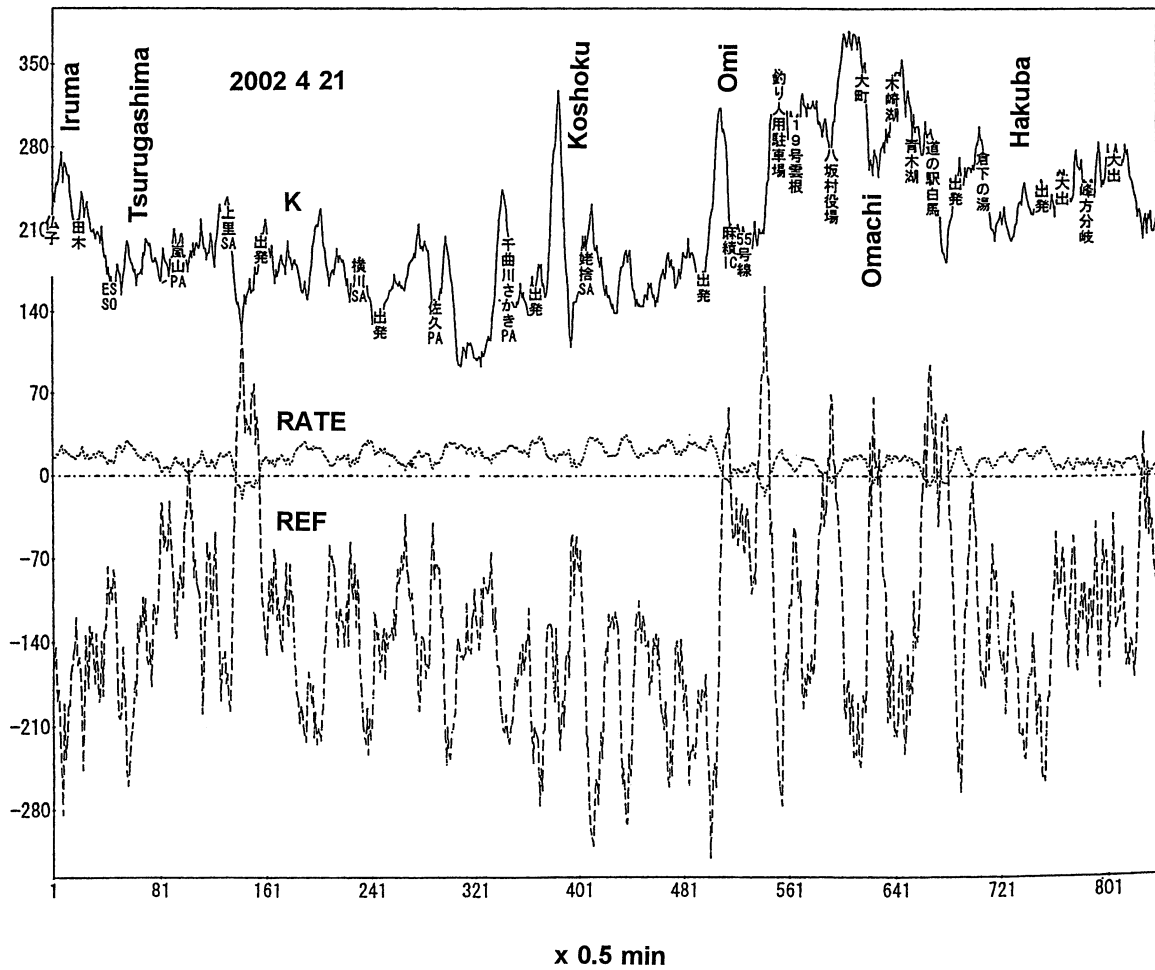


Fig. 6. Example of the output of the RE-100, i.e.,  $K$ ,  $REF$ , and  $RATE$  versus elapsed time. This is the profile obtained from the car. The abscissa is travel-time, which corresponds to a place along the road from Iruma City, Saitama Prefecture to Hakuba Village, Nagano Prefecture, as shown in Fig 5.

The data adopted for the above test are from measurements taken aboard a Shinkansen train and a car. Figs. 4 and 5 show the route maps. The  $K$ ,  $REF$ , and  $RATE$  data obtained aboard the car along the route presented in Fig. 5 are shown in Fig. 6. RE-100 detects gamma-rays with a NaI scintillator and counts events detected every 30 sec. The counting data are stored in the memory. The counting data logger is designed to store only those  $K$ ,  $REF$ , and  $RATE$  at every 30 sec. Moreover, the data values are summarized as moving-average values with a constant length of time-window. We decided on the time length of 5 min as discussed in the next section.

Figures 7 and 8 are graphs plotting  $B$  versus  $K$ , which are defined in Section 2. Both graphs show a clear statistical correlation between  $^{214}\text{Bi}$  and  $^{40}\text{K}$  radiation. The linear relations are formulated as fol-

lows:

$$B = 3.14K + 109.4 \quad (5)$$

for the survey data obtained aboard a train,

$$B = 2.74K + 186.0 \quad (6)$$

for that obtained aboard a car. The above functions of  $B$  are empirical forms of  $f(K)$  in Eq. (1). Generally, the function  $f(K)$  is written as

$$f(K) = aK + b. \quad (7)$$

Here,  $a$  takes a value of approximately 3.0. The value of  $b$  changes according to the measurement conditions: height of measurement above the ground, and geological setting, etc. Although it is better to adopt realistic values of  $a$  and  $b$  for each observation, we adopt hereafter the values given by Eq. (3) for sim-

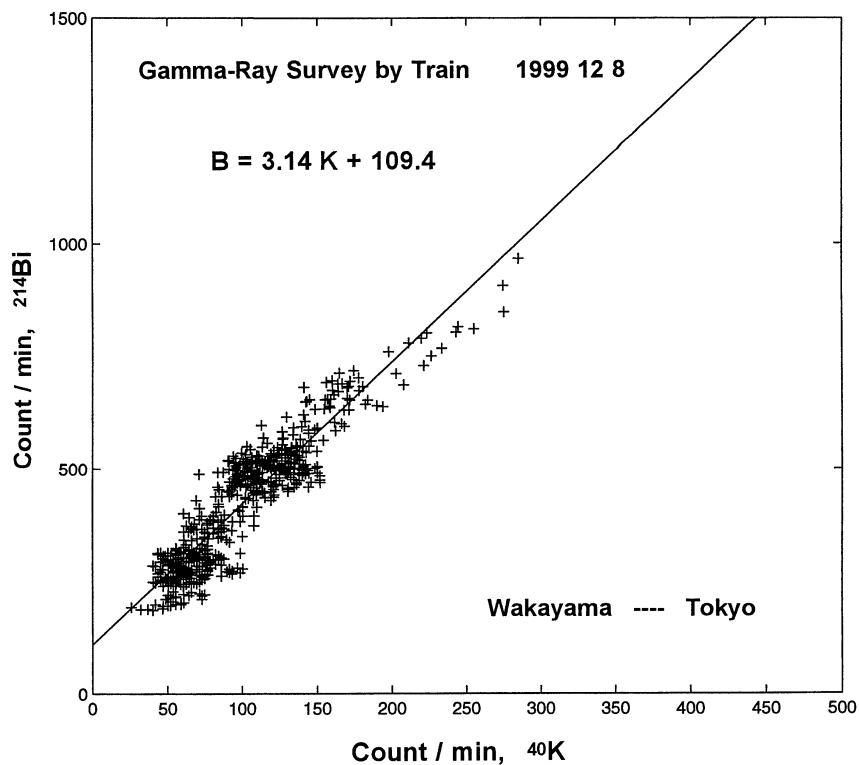


Fig. 7. Correlation between  $B$  (Bismas-214) and  $K$  (Potassium-40) for survey by train.  $B$  is calculated from  $K$ ,  $REF$ , and  $RATE$  (See text). The survey route is the railroad from Wakayama to Tokyo as shown in Fig. 4.

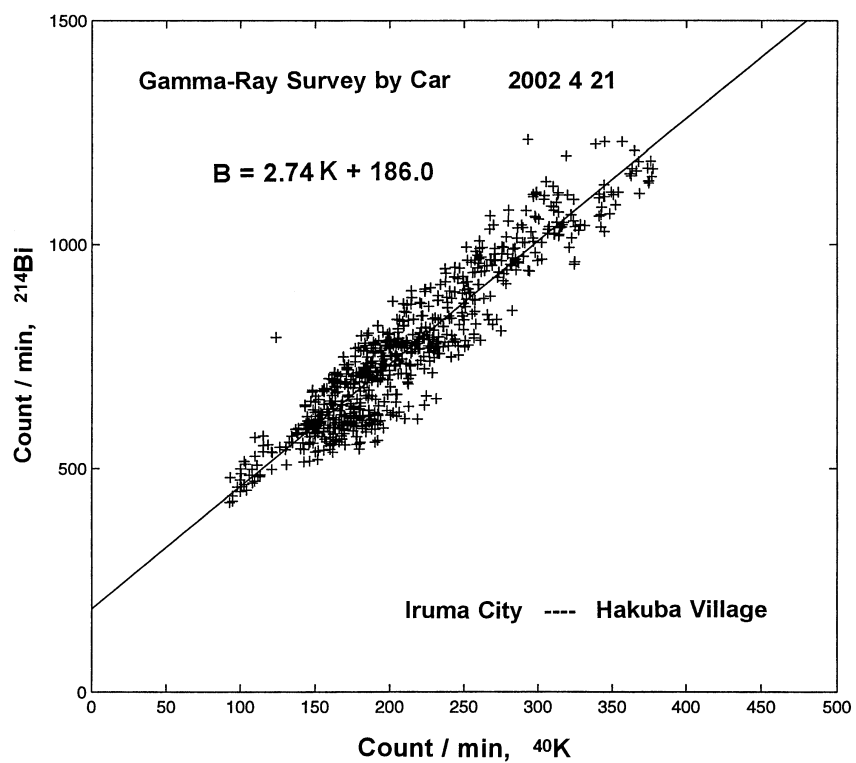


Fig. 8. Correlation between  $B$  (Bismas-214) and  $K$  (Potassium-40) for survey undertaken by car. The route is from Iruma City, Saitama Prefecture to Hakuba Village, Nagano Prefecture, central Japan, as shown in Fig. 5.

plicity. The value  $a$  is considered to be approximately valid under any circumstances. The value  $b$  is considered to be a kind of simple offset for all data points, and to slightly affect the trend of the profile.

The counting values of the parameters  $K$ ,  $B$ , and  $REF$  have a unit of count/min throughout this paper.

#### 4. Observations at a fixed point

The long-term monitoring of crustal activity related to the premonitory process of a large earthquake is the main purpose of developing the gamma-ray observation system. The RE-100 radon emanometer has not enough memory to accumulate long-running observation data. The method we adopt for RE-100 is to repeat short-term observations or conduct semi-continuous observations.

A wooden house in the countryside was adopted as the semi-continuous observation station, because many modern laboratories in cities are made of concrete, which has large amounts of noisy gamma-ray source Potassium-40. It is located in Inagawa Town, Hyogo Prefecture, close to the seismic active region from Kyoto to Kobe (See Fig. 4). The instrument was set at an upstairs room of the wooden two-story house. The height from ground level is about 2.5 m.

An example of data,  $REF$ , obtained with RE-100 is shown in Fig. 9. The observation period is 15 hours, which corresponds to the maximum memory of 64 kB.  $REF$  is counted at 30 sec intervals. The original raw data are shown in the bottom graph. The value of  $REF$  changes rapidly with time. It is suggested that gamma-ray radiation is generated by a random process.

To detect some gamma-ray activity of a certain duration, we integrate the time series of  $REF$  to suppress fluctuations. The upper graphs show the integrated  $REF$ , taking running mean over the preceding period, of which time-length are given in numerals in the figure. The standard deviation of each case of time-window for integration is reduced by 30% of the original data beyond about 5 min of the time-length of the window.

Some predominant short-period impulsive fluctuations should be detected even after the integration process. An example of the impulse is shown in Fig. 9 with the mark X. When the time-window is as short as 3 min, the impulse is still predominant. However, for the 5-min window, the impulse is sup-

pressed, but can be detected clearly. The optimal time-window is around 5 min. We adopt this for every measurement in this paper.

Semi-continuous observations with RE-100 at the wooden house have been carried out about three times in a year for more than eight years. A single observation captures data during 15 hours. The mean value of  $REF$  and  $K$  for each observation and their standard deviations are shown with elapsed time in Fig. 10. Every piece of data of the standard deviation is almost constant in a long-term trend with some fluctuations. This suggests that short-term fluctuations of the gamma-ray radiation process and instrumental noise are very stable over time.

In this figure, we notice a long-term increasing trend for  $REF$  after around the end of 2001, in contrast to a constant trend for  $K$ . The increasing rate is 16 count/min/year. This suggests that the radon gas emissions at Inagawa increased in recent years. The above change in  $REF$  is possibly related to recent anomalous crustal activity found in the Kinki region (Tsukuda, 2007).

After 2005, we replaced the old RE-100 instrument with a new one. Semi-stationary observations continued, conducting parallel observations using both instruments to confirm differences in radon induced gamma-ray detection between the devices. After differences between the instruments are clarified, the data on temporal changes following this study will be presented in the future.

#### 5. Observations on a vehicle along a fixed survey line - in the case of survey on a Shinkansen-train

The RE-100 mobile radon emanometer was originally designed for gamma ray surveys on foot along a line on the ground. However, trains and cars are convenient carriers of the emanometry device when we need to cover a long distance on a fixed survey route. Repeated surveys along railways or roads have been conducted to detect any statistic properties of radon emanation in the air just above the ground. Some examples of observed data have been presented in the report paper: Tsukuda (2006a) for the survey conducted by train, Tsukuda (2006b) for that conducted by car.

We present below examples of measurements

## Gamma-Ray Observation at Inagawa Town 1998 7 24

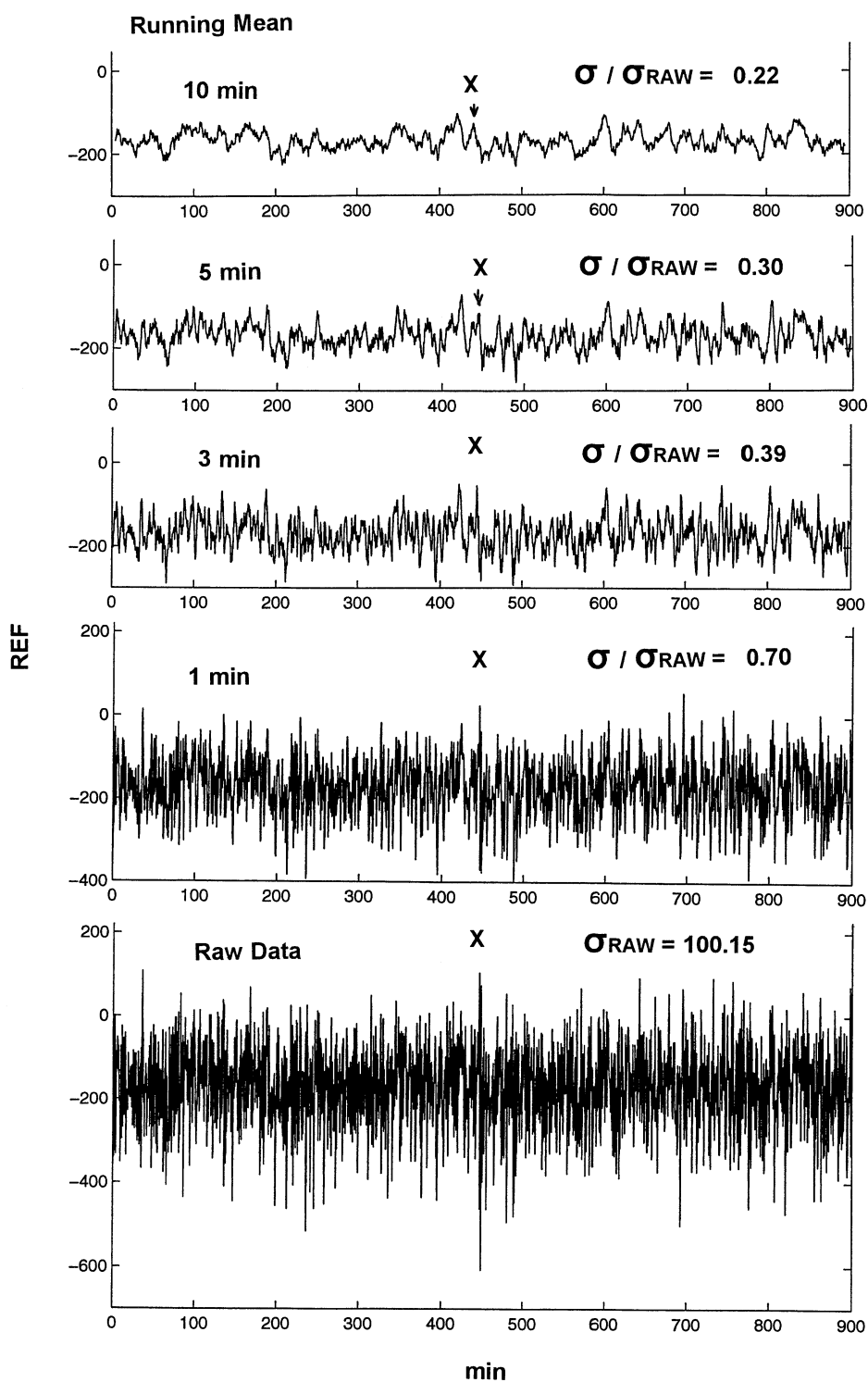


Fig. 9. An example of *REF* measured during the 15-hour period at a wooden house in Inagawa Town, Hyogo Prefecture. The bottom shows the original counting value every 30 sec. The upper figures are the graph of running mean values with each time window as shown in numerals. Each mean value calculated for the preceding period is plotted at every 30 sec. The marks with X denote the most predominant impulsive fluctuation.  $\sigma$  denotes the standard deviation of each *REF* dataset.

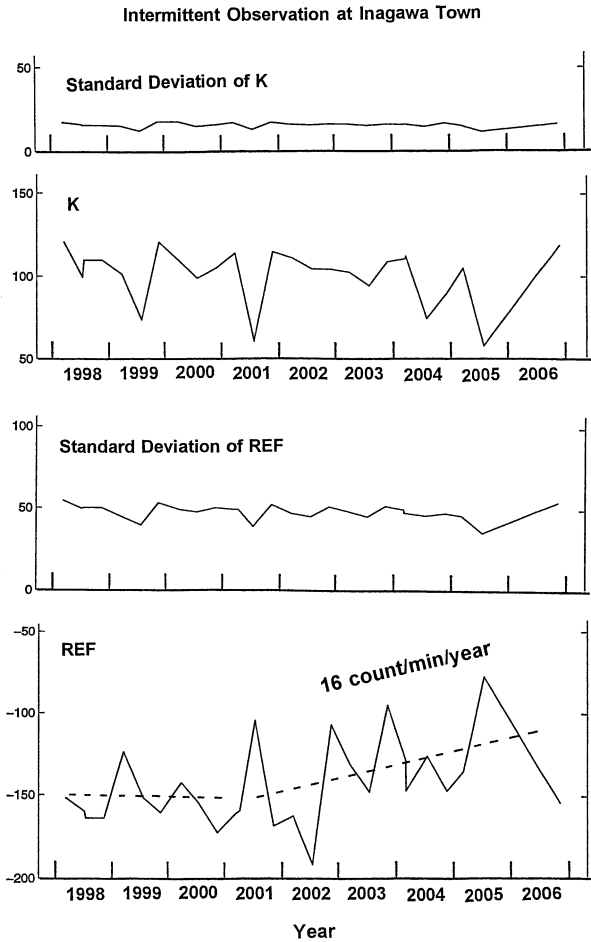


Fig. 10.  $K$  and relative  $REF$  with their standard deviation from semi-stationary observation of gamma-ray at Inagawa-town, Hyogo Prefecture. Each data point represents averages of a 15-hour measurement period.

obtained aboard a Shinkansen train. The Shinkansen train in Japan is a bullet train, which travels at a speed of more than 200 km/hr. We take the New Tokaido Line starting from Shin-Osaka station to Tokyo station (Fig. 4). Repeated measurements are carried out on the Kodama train from Kyoto to Tokyo stopping at all stations. The profiles for  $K$  and  $REF$  from Kyoto to Tokyo against travel time are obtained.

The first-generation RE-100 was used until the summer of 2005. For this paper, data of 23 profiles were analyzed (Table 2). For ease of comparison, we use relative  $REF$ , which is defined as the value of  $REF$  after subtracting the mean of the values of the time series from the original value.

To suppress random fluctuations in the profile,

the time series  $K$  and  $REF$  are added together (stacked) at each time point and divided by the number of profiles. We get a mean profile, which here is called a stacked profile. Figure 11 shows the stacked profile for all 23 events.

Some peaks found in the  $K$  or channel  $^{40}\text{K}$  profile occur at tunnels. Gamma-ray radiation tends to be high in tunnels because it comes not only from the ground but from the wall and ceiling of the tunnel. The main tunnels are: Otowa-yama tunnel near Kyoto (5 km long), Sekigahara tunnel between Maibara and Gifu-Hashima stations (3 km long), Makinohara tunnel between Kakegawa and Shizuoka (3 km long), Yui tunnel between Shizuoka and Atami (7 km long), and Tan'na tunnel near Atami (8 km long).

The peaks of  $REF$  also correspond to those of  $K$  except near the Kyoto region. Because radon gas coming from underground is confined in tunnel air for a while without dispersing into the outside open air, the probability of detecting radon gas there is higher than on flat open ground.

The time schedules of Shinkansen trains are quite regular and we can safely assume travel time corresponds exactly to the place the train passes at a particular time. However, strictly, the Shinkansen time diagram has changed over time. As shown in Table 2, the total time length of data has decreased by about 10 minutes. For this reason the widths of some of the peaks of  $K$  in tunnels are somewhat broader.

In Fig. 12, each profile of the relative  $REF$  is presented. The standard deviation  $\sigma$  of  $REF$  for each profile is calculated: 2 and 3 $\sigma$  levels are shown by the line with note +. The anomaly the relative  $REF$  exceeding 3 $\sigma$  occurs in the region between Kyoto and Maibara, near Gifu-Hashima, near Nagoya, between Kakegawa and Shizuoka, and near Atami. The three cases between Kakegawa and Atami occur in tunnels.

Strictly, the standard deviation should be calculated region by region because the radon concentration level is dependent on the geologic setting of the region. Here, we calculate it for the entire data for simplicity.

The most noticeable group of anomalies is located between Kyoto and Maibara. As shown in Fig. 13, the number of anomalies with high relative  $REF$  exceeds 3 $\sigma$  is 7 out of the total 23 cases, i.e. 30%.

Table 2. List of gamma-ray surveys undertaken by Shinkansen train from Kyoto to Tokyo.  
Data: survey event number, date of survey, starting time at Kyoto, travel time from Kyoto to Tokyo, mean value of  $K$ ,  $REF$ , and  $RATE$ , and standard deviation of  $K$ ,  $REF$ , and  $RATE$ .

N	Y	M	D	Starting T. H:M	Travel T. min.	$K$	$K$ S.D.	$REF$	$REF$ S.D.	$RATE$	$RATE$ S.D.
1	1999	12	8	13:17	234	83.30	30.86	-169.70	67.34	32.36	14.30
2	2000	3	29	12:17	233	86.21	34.43	-162.66	73.22	30.84	15.11
3	2000	4	13	13:16	234	84.28	35.88	-180.95	56.94	34.34	12.25
4	2000	7	15	13:16	233	84.90	35.18	-170.19	57.80	32.49	13.07
5	2000	8	11	12:17	234	63.80	21.56	-158.56	51.33	33.15	12.10
6	2000	11	15	17:18	232	87.01	34.47	-175.28	58.34	32.83	13.04
7	2001	3	21	15:17	233	71.66	29.02	-175.45	54.03	35.40	12.74
8	2001	4	5	17:18	233	65.47	25.16	-168.86	65.58	35.41	15.08
9	2001	4	11	12:17	234	68.96	30.27	-167.20	58.33	34.51	13.99
10	2001	7	18	12:17	233	40.21	19.73	-111.56	69.44	27.88	17.82
11	2001	8	10	10:17	235	94.55	39.21	-187.39	57.20	33.98	12.76
12	2001	11	13	16:17	229	104.69	41.00	-176.76	53.44	30.58	11.49
13	2001	12	28	14:17	231	88.60	35.51	-192.40	53.70	35.45	11.87
14	2002	3	21	13:17	228	92.33	36.22	-160.01	66.26	29.33	13.68
15	2002	7	23	12:17	229	81.07	32.35	-191.47	53.67	36.71	12.41
16	2002	11	21	13:17	229	87.25	37.53	-172.79	53.22	32.42	11.95
17	2003	3	23	13:17	229	68.04	30.84	-179.78	53.07	37.12	13.02
18	2003	10	9	15:37	225	93.85	40.05	-165.07	60.00	30.50	13.47
19	2003	11	14	12:40	223	88.38	34.10	-129.85	67.87	24.85	14.17
20	2004	3	12	12:40	223	88.61	33.70	-144.19	57.58	26.70	11.60
21	2004	7	27	12:40	223	55.75	29.07	-136.37	65.41	30.73	16.13
22	2004	11	28	12:40	223	54.29	25.83	-131.90	59.37	29.92	14.40
23	2005	3	18	12:39	224	70.79	28.49	-129.23	68.88	26.74	15.18

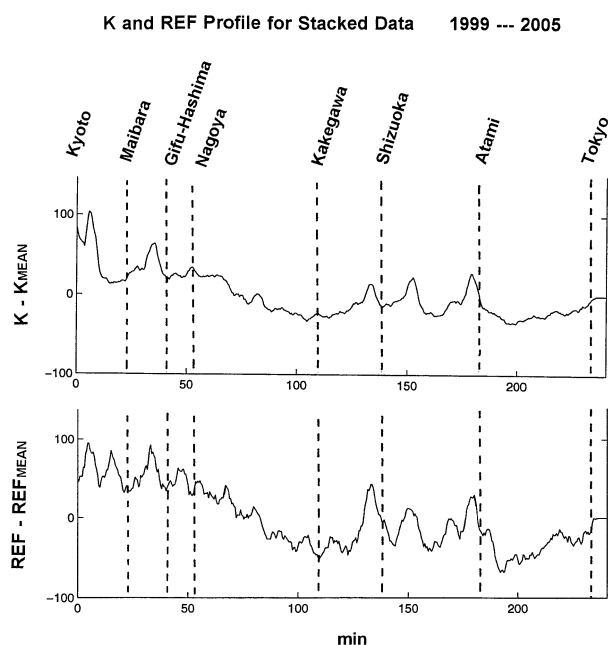


Fig. 11. Stacked relative  $REF$  profile for repeated surveys by Shinkansen train. Abscissa is travel-time, which corresponds to the location on the railway.  $REF$  data are summed and divided by the number of events, 23 at each travel-time.

Furthermore, anomalies occurred particularly around the year 2000. Taking five cases that occurred near Kyoto, the percentage is 22%. Radon emanation in a region near Kyoto is relatively high compared to other regions. This may have some relation to recent anomalous crustal activity in the Kinki district (Tsukuda, 2007).

However, it is possible the radon concentration near Kyoto is due to a special geologic setting supplying large quantities of radon. The correct answer will be obtained by continuing this study into the future.

## 6. Discussion and concluding remarks

Yasuoka (2006) made long-term continuous observations of radon at Kobe, and found an anomalous rise of the radon concentration in the air before one month of the occurrence of the 1995 Hyogo-ken Nanbu earthquake. This result encourages us to monitor the radon concentration in the air.

This paper presents a technique for a gamma-ray survey to monitor crustal activity and to verify the method. The main results are as follows:

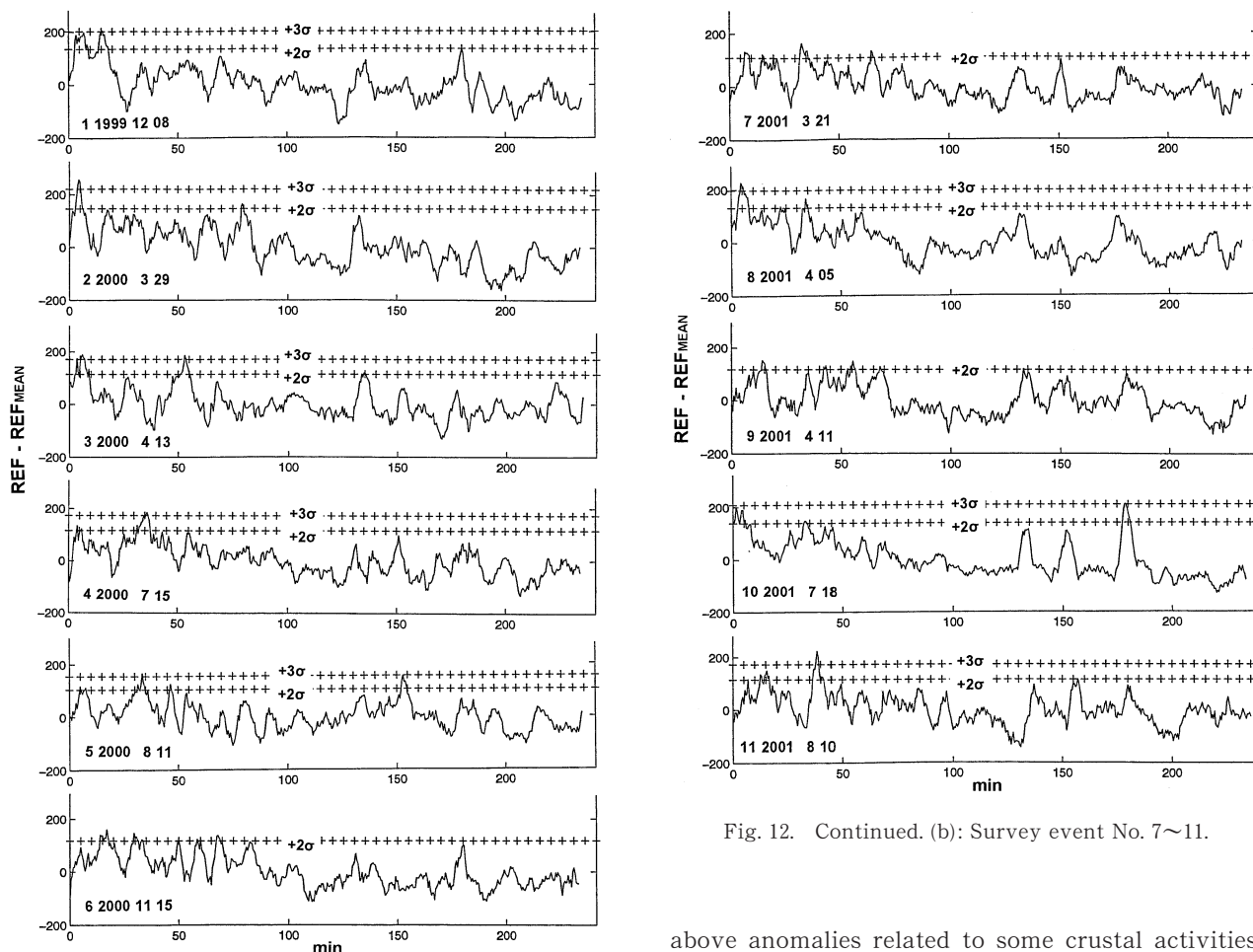


Fig. 12. Individual relative *REF* profiles for repeated surveys undertaken by Shinkansen train. (a): Survey event No. 1~6. The numeral attached to the profile corresponds to the event number listed in Table 2.

Fig. 12. Continued. (b): Survey event No. 7~11.

- 1) A radon emanometry method is proposed and applied to real data. The validity of this method is clearly confirmed provided data are accumulated from repeated measurements.
- 2) Semi-stationary observations were carried out for eight years at Inagawa, Hyogo Prefecture. It was found that radon emanation increased over time from around the end of 2001 with a rate of 16/count /min/year.
- 3) The stacking method was applied to railway observation data. Anomalous high radon emanations were found at some particular regions near Kyoto. The occurrence rate there is more than 22% of all surveys. There is a possibility of anomalous radon activity around Kyoto.

To elucidate the mechanism and details of the

above anomalies related to some crustal activities, we will continue the study as presented in this paper. The instrument we have been using recently is a new second-generation device because the first-generation device was rather old with fading resolving power. We are conducting parallel observations repeatedly and are collecting data to calibrate the instruments. After completing calibration, we will be able to present data with an observation period that is longer than in this paper.

#### Acknowledgements

The author is indebted to many persons who introduced the study of radioactivity, and provided facilities and calibration tools for gamma-ray measurements. Late Professor emeritus of Ritsumeikan University, Kazuo Mino showed the importance of gamma ray surveys. Dr. Harumi Araki gave guidance on gamma ray measurements. Mr. Masao Tanaka and Naoki Tanaka at Inagawa Town in Hyogo Prefecture, Mr. Masanori Obuchi and Mr. Norio Nakamura at Ohyo Koken Kogyo Co. Ltd., Fussa City, Tokyo were helpful in making various

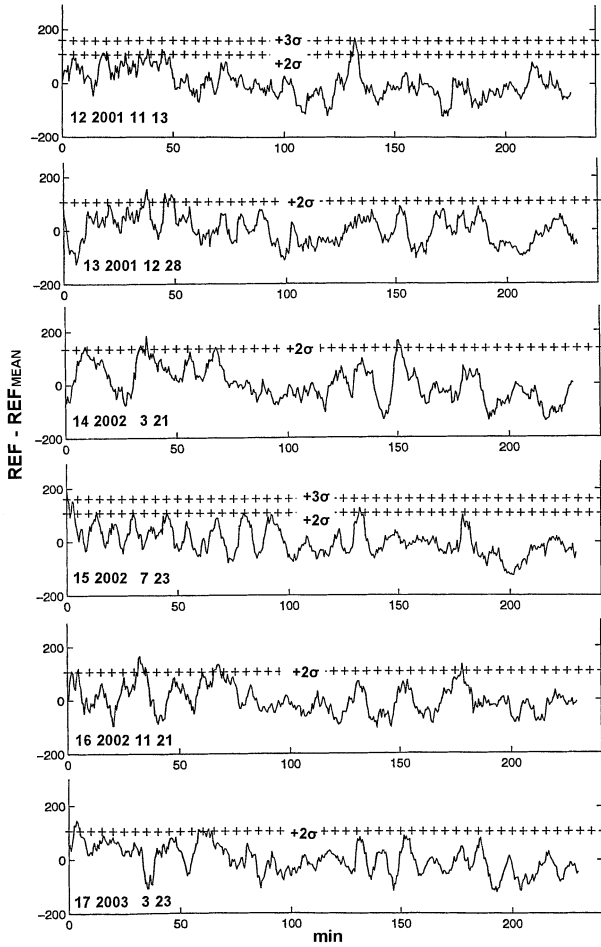


Fig. 12. Continued. (c): Survey event No. 12~17.

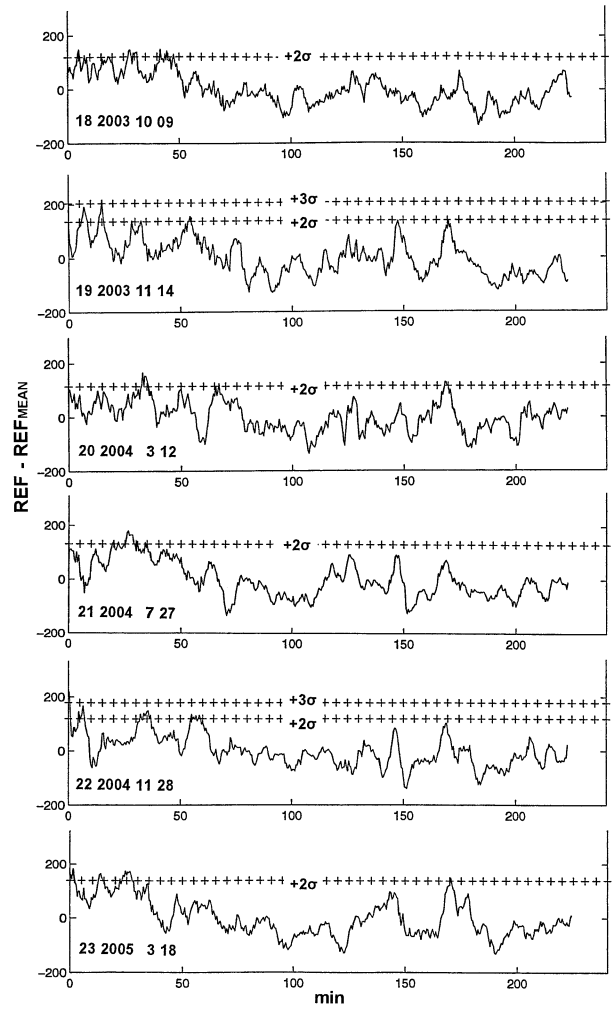


Fig. 12. Continued. (d): Survey event No. 18~23.

experiments. The author's sincere thanks are extended to Prof. Hiroaki Tsukahara of Shinshu University for critically reviewing the manuscript.

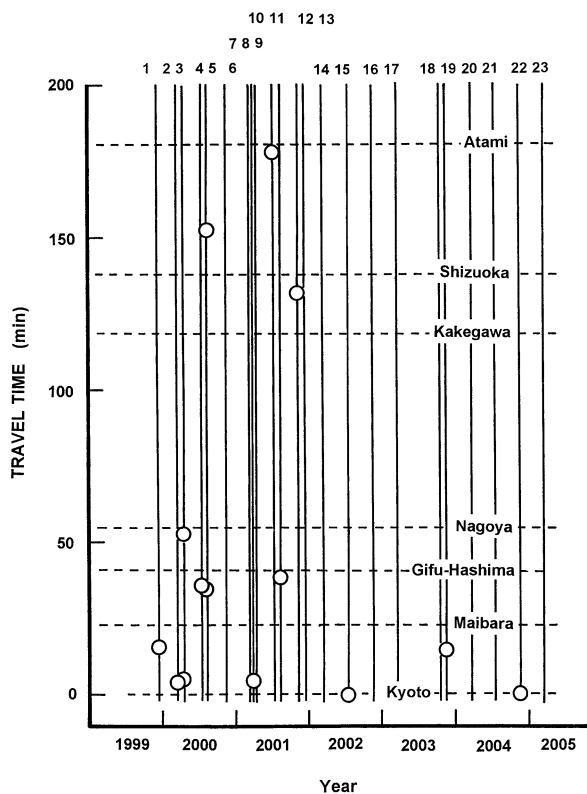


Fig. 13. Space-time diagram for anomalies of radon emanations detected by observations on Shinkansen trains. An anomaly is defined to occur when the relative REF exceeds three times the standard deviation. The open circles indicate the location on the New-Tokaido Line and the date of observation on which the anomalies occurred. Numerals attached to vertical lines are event numbers listed in Table 2.

**References**

Araki, H., 1994, Airborne radon emanometry, *Journal of the Japan Society of Photogrammetry and Remote Sensing*, **33**, No. 4, 32-57 (in Japanese).  
 Araki, H., 1996a, The survey of crustal movements by radon observation (Part 1), *Journal of the Japan Society of Photogrammetry and Remote Sensing*, **35**, No. 5, 59-66 (in Japanese).  
 Araki, H., 1996b, The survey of crustal movements by radon observation (Part 2), *Journal of the Japan Society of Photogrammetry and Remote Sensing*, **35**, No. 6, 34-47 (in Japanese).  
 Evans, R.D. and C. Goodman, 1941, Radioactivity of rocks, *Bull. Geol. Soc. Am.*, **52**, 459-490.  
 Hatuda, Z., 1953, Radon content and its change in soil air near ground surface, *Mem. Coll. Sci. Univ. Kyoto*, **20b**, No. 4, 227-306.  
 Igarashi, G., S. Saeki, N. Takahata, K. Sumikawa, S. Tasaka, Y. Sasaki, M. Takahashi and Y. Sano, 1995, Ground-

water radon anomaly before the Kobe earthquake in Japan, *Science*, **269**, 60-61.  
 Katsura, I, S. Nakao, Y. Kishimoto, T. Shibutani, K. Mino, R. Nishida, 1989, Continuous measurement of  $\gamma$ -ray count rate in an observation vault at Tottori, *Zisin 2*, **42**, 299-310 (in Japanese with English abstract).  
 Nakao, S., Y. Kishimoto, T. Shibutani, K. Mino, R. Nishida, and I. Katsura, 1987, Continuous observation of  $\gamma$ -ray intensity in an observation vault (I), *Annual. Dis. Prev. Res. Inst.*, No. **30 B-1**, 57-65 (in Japanese with English abstract).  
 Okabe, S., 1956, Time variation of the atmospheric radon-content near the ground surface with relation to some geophysical phenomena, *Mem. Coll. Sci. Univ. Kyoto Ser. A*, **28 (2)**, 99-115.  
 Sadahiro T., and K. Mino, 1980, The  $\gamma$ -ray intensity around active faults (I), *Zisin 2*, **33**, 51-70 (in Japanese with English abstract).  
 Ten, T.L., 1980, Some recent studies on groundwater radon content as an earthquake precursor, *J. Geophys. Res.*, **86**, 3089-3099.  
 Tsukuda, T., K. Gotoh and O. Sato, 2005, Deep groundwater discharge and ground surface phenomena, *Bull. Earthq. Res. Inst., Univ Tokyo*, **80**, 1-27.  
 Tsukuda, 2006a, Gamma-ray survey for crustal activity by train, *Annual Report of 2006: Cooperative Study on Earthquake Prediction of Inland Earthquakes*, *Earthq. Res. Inst., Univ Tokyo*, 78-109 (in Japanese).  
 Tsukuda, 2006b, Gamma-ray survey for crustal activity by car, *Annual Report of 2006: Cooperative Study on Earthquake Prediction of Inland Earthquakes*, *Earthq. Res. Inst., Univ Tokyo*, 110-135 (in Japanese).  
 Tsukuda, 2007, Recent water temperature rise at an artesian well and crustal activity changes in Kinki District at the Niigata-Kobe Tectonic Zone, *PROGRAMME and ABSTRACTS, Seism. Soc. Japan, 2007 Fall Meeting D22-11*, 133 (in Japanese).  
 Ulomov, V.I. and B.Z. Mavashev, 1971, Forerunners of the Tashkent earthquakes, *Izv. Akad. Nauk Uzb., SSR*, 188-200.  
 Wakita, H., Y. Nakamura, K. Notsu, M. Noguchi and T. Asada, 1980, Radon anomaly: A possible precursor of the 1978 Izu-Oshima-kinkai earthquake, *Science*, **207**, 882-883.  
 Yamauchi, T. and M. Shimo, 1982, Radon concentration in galleries and its relation to the earthquake occurrence, *Zisin 2*, **21**, 1064-1072 (in Japanese with English abstract).  
 Yamauchi, T., M. Shimo and R. Miyazima, 1988, Variation of radon concentration in air in observation tunnels at Toyohashi and Kikugawa, Tokai area Japan, *Zisin 2*, **41**, 335-342 (in Japanese with English abstract).  
 Yasuoka, Y., G. Igarashi, T. Ishikawa, S. Tokonami, and M. Shionogi, 2006, Evidence of precursor phenomena in the Kobe earthquake obtained from atmospheric radon concentration, *Appl. Geochem.*, **21**, 1064-1072.

(Received May 16, 2008)

(Accepted September 9, 2008)